Transient loading of CD34+ hematopoietic progenitor cells with polystyrene nanoparticles

Peer-reviewed author version

DEVILLE, Sarah; Hadiwikarta, Wahyu Wijaya; SMISDOM, Nick; WATHIONG, Bart; AMELOOT, Marcel; Nelissen, Inge & HOOYBERGHS, Jef (2016) Transient loading of CD34+ hematopoietic progenitor cells with polystyrene nanoparticles. In: International Journal of Nanomedicine, 12, pag. 459-472.

DOI: 10.2147/IJN.S119407
Handle: http://hdl.handle.net/1942/22623

Transient loading of CD34+ hematopoietic progenitor cells with polystyrene nanoparticles

Sarah Deville[1,2]

Wahyu Wijaya Hadiwikarta[1]

Nick Smisdom[1,2]

Bart Wathiong[1]

Marcel Ameloot[2]

Inge Nelissen[1]

Jef Hooyberghs[1,3]

[1]Flemish Institute for Technological Research, Boeretang 200, 2400 Mol, Belgium; [2]Biomedical Research Institute, Hasselt University, Agoralaan C, 3590 Diepenbeek, Belgium; [3]Theoretical Physics, Hasselt University, Agoralaan D, 3590 Diepenbeek, Belgium

Correspondence: Jef Hooyberghs

Flemish Institute for Technological Research

Industriezone Vlasmeer 7

2400 Mol, Belgium

Tel +32 14 33 52 77

Fax +32 14 58 05 23

Email jef.hooyberghs@vito.be

Abstract: $CD34^+$ hematopoietic progenitor cells (HPCs) offer great opportunities to develop new treatments for numerous malignant and non-malignant diseases. Nanoparticle (NP)-based strategies can further enhance this potential, therefore a thorough understanding of the loading behavior of HPCs towards NPs is essential to a successful application. Present study focusses on the interaction kinetics of 40-nm sized carboxylated polystyrene (PS) NPs with HPCs. Interestingly, a transient association of the NPs with HPCs is observed, reaching a maximum within one hour and declining afterwards. This behavior is not seen in dendritic cells (CD34-DCs) differentiated from HPCs, which display a monotonic increase in NP load. We demonstrate that this transient interaction requires an energy-dependent cellular process, suggesting active loading and release of NPs by HPCs. This novel observation offers a unique approach to transiently equip HPCs. A simple theoretical approach modelling NP loading and release is presented, contributing to a framework to describe this phenomenon.

Keywords: nanoparticles; hematopoietic progenitor cells; dendritic cells; uptake; release.

Introduction

Hematopoietic stem cells (HSCs) and hematopoietic progenitor cells (HPCs) offer great opportunities to develop new treatments for numerous malignant and non-malignant diseases. Their ability for self-renewal and to differentiate into all blood lineages is nowadays utilized for stem cell therapies.[1] New strategies utilizing viral vectors or, more recently, nanoparticles (NPs) attempt to manipulate these cell types, or track or guide them to the place of action.[2,3] The usage of NPs for HSCs- and HPCs-based (and concurrent and/or associated gene) therapies has received considerable attention as it can circumvent efficacy and safety issues of the classical vehicles.[4,5]

Due to their small size, NPs possess new chemical and physical properties as compared to the corresponding bulk material. Since NP size can be in the same order of magnitude as biomolecules and viruses, they are capable to enter cells and interact with the cellular

machinery.[6,7] In the medical field, NP-based strategies offering unprecedented applications are therefore increasingly preferred over the traditional diagnostic and therapeutic methods. Indeed, (i) NPs can easily be loaded with imaging agents, bio-active molecules and drugs due to their large surface area and inner volume, (ii) NPs' surfaces can be easily functionalized and as such have the possibility to allow for specific (sub)cellular targeting, (iii) NPs display an enhanced circulation time in the blood compared to traditional therapeutics, and (iv) NPs can be made multifunctional to exert both diagnostic and therapeutic actions.[8] These features enable a more efficient targeting, guidance and actuation towards HSCs and HPCs. As a result, the utilization of NPs holds great promise for improved cell and gene therapies.[2]

Recent studies have focused on directing NPs towards HSCs; however, the use of NPs in combination with HSCs is not yet fully exploited. HSCs have been labelled with superparamagnetic iron oxide (SPIO) NPs and gadolinium oxide (Gd_2O_3) NPs for MRI contrast enhancement and cell tracking.[9-12] Additionally, the delivery of peptide nucleic acids by poly(lactic-co-glycolic acid) (PLGA) NPs for genome editing in HSCs is currently under investigation.[13,14] In the available knowledge, limited attention is payed to the loading behavior of HSCs and HPCs with NPs, not to mention the kinetics involved. Since this determines the efficacy and safety of nanotechnology-based applications, it is definitely worthwhile to consider these aspects in more detail.

In the present study, we investigated the interaction, which includes the association with the cell membrane and uptake, and kinetics of human cord blood-derived $CD34^+$ HPCs with well-defined, 40-nm sized yellow-green fluorescently dyed carboxylated polystyrene (YG-PS) NPs. PS NPs are of medical interest as multifunctional carriers for therapy.[15,16] They are also commonly used as a model NP to study the interaction with biological systems because of their commercial availability, high quality, and large range of sizes and surface chemistries.[17] A unique transient loading behavior was observed, suggesting active loading and release of the YG-PS NPs by HPCs. This behavior was compared with the YG-PS NPs' interaction with myeloid-type dendritic cells (CD34-

DCs). DCs are derived by differentiation from $CD34^+$ HPCs and play a key role in initiating, directing and controlling both the innate and adaptive immune response.[18] The CD34-DCs did not exhibit the transient loading.

Material and methods

Isolation and culture of $CD34^+$ HPCs and CD34-DCs

$CD34^+$ HPC isolation and culture procedures have been described previously.[19] Briefly, human cord blood samples were collected from umbilical blood vessels of placentas of full-term infants, born at the Heilig Hart hospital in Mol, Belgium and the St. Dimpna hospital in Geel, Belgium. Informed consent was given by the mothers and the study was approved by the ethical commission of both hospitals. Mononuclear cells were separated from the cord blood by density gradient centrifugation (Ficoll-Paque™ plus, GE Healthcare, Uppsala, Sweden). Subsequently, $CD34^+$ HPCs were extracted using positive immunomagnetic selection (EasySep® human CD34 positive selection kit, Stemcell Technologies, Grenoble, France) according to the manufacturer's guidelines. 95 ± 3 % (n = 3) of the purified HPCs were positive for CD34. HPCs were cultured for 12 days in Iscove's Modified Dulbecco's Medium (IMDM, Gibco, Paisley, UK) supplemented with 10% fetal bovine serum (FBS, PAA laboratories, Pasching, Austria), 2% penicillin/streptomycin (P/S, 5000 U/ml-5000 µg/ml, Gibco) and 1% bovine serum albumin (BSA, Sigma-Aldrich, Steinheim, Germany) in the presence of tumor necrosis factor alpha (TNF-α, 250 U/ml, Roche applied science, Upper Bavaria, Germany), granulocyte-macrophage colony-stimulating factor (GM-CSF, 5000 U/ml, Gentaur, Brussels, Belgium), stem cell factor (SCF, 5 U/ml, Biosource, Nivelles, Belgium) and interleukin 4 (IL-4, 1000 U/ml, Biosource) to induce proliferation and differentiation towards immature CD34-DCs.

Nanoparticles and characterization

Yellow-green (λ^{ex} 505 nm, λ^{em} 515 nm) 40-nm carboxylated polystyrene (YG-PS) NPs were purchased from Molecular Probes (Invitrogen, Merelbeke, Belgium). NP dispersions were prepared by diluting the concentrated stock solutions in complete cell culture medium (CCM) – which is IMDM supplemented with 10% FBS, 2% P/S and 1% BSA – immediately before addition to the cells. YG-PS NPs were characterized in both water and CCM by means of nanoparticle tracking analysis (NTA) using a Nanosight NS500 instrument (NanoSight Ltd., Wiltshire, United Kingdom) and zeta potential determination using ZetaPALS (Brookhaven instruments corporation, Holtsville, USA).

Dialysis of nanoparticles

YG-PS NPs stock solutions were dialyzed using Slide-A-Lyzer® Mini dialysis units and Slide-A-Lyzer® Gamma Irradiated dialysis cassettes (10 000 MWCO Plus, Thermo Scientific, Rockford, USA) against citric acid – phosphate buffers with a different acidity (pH 5 – pH 7). The fluorescence intensity of the dialysate was monitored using a fluorescence spectrophotometer (LS55, Perkin Elmer, Waltham, Massachusetts, USA). BODIPY® FL (4,4-Difluoro-5,7-Dimethyl-4-Bora-3a,4a-Diaza-s-Indacene-3-Propionic Acid) (Life Technologies) was used for free dye as a control in the dialysis experiments. In order to obtain pre-dialyzed PS NPs or free dye for the cell exposure experiments, YG-PS NPs were dialyzed against citric acid – phosphate buffer with pH 7 for 48 hours at 37°C. For the cell exposure experiments, the dialysate containing only the dye was further diluted and used to expose the cells. This dilution, taking into account the additional dilution due to the dialysis, was performed to obtain an amount of dye equal to the amount of free dye present in the YG-PS NP solution used in the cell experiments.

Flow cytometry

NP loading of the cells was evaluated by means of flow cytometry (FACS Calibur™, Becton Dickinson, San Jose, California, USA). HPCs and CD34-DCs were seeded at a density of 5×10^4 cells/well in 96-well plates and immediately exposed to YG-PS NPs at 37°C and 5% CO_2 until

analysis. For the experiments performed at 4°C, cells were cooled down in the refrigerator (either one hour before exposure or after one hour of exposure) and handled on ice. After the desired exposure time, cells were transferred to polystyrene tubes (Becton Dickinson), washed three times with phosphate buffer saline (PBS, without Ca^{2+} and Mg^{2+}, Gibco) to remove loosely adherent NPs and collected by centrifugation. Flow cytometric analyses were performed on fresh cell suspensions directly after the final collection. HPCs and CD34-DCs were identified by light scatter using gates to exclude dead cells and cell debris. For each sample 10,000 events in the gated region were acquired. Light scattering profiles and fluorescence histograms were evaluated using CellQuest™ (Becton Dickinson) and home-written MATLAB routines (The Mathworks, Eindhoven, The Netherlands). NP loading was evaluated by the geometric mean of the fluorescence intensity (GMFI) distributions. The same photomultiplier voltages and compensation settings were applied for HPCs and CD34-DCs in order to allow comparison between both.

Confocal microscopy

HPCs and CD34-DCs were exposed to 50 µg ml^{-1} YG-PS NPs for 1, 2, 3, 4, 6 or 24 hours at 37°C and 5% CO_2. After exposure, cells were washed with PBS for three times and cell membranes were labelled with 5 µg/ml Alexa Fluor® 555 conjugated wheat germ agglutinin (WGA, Invitrogen) at 4°C for 30 minutes. After washing, cells were fixed with 4% formalin solution (Sigma-Aldrich) and transferred to a microscope slide by means of cytocentrifugation (Tharmac Cellspin II, Tharmac, Waldsolms, Germany). Cells were mounted with Vectashield® mounting medium containing DAPI (Vector Laboratories, Peterborough, United Kingdom). Images were acquired using an epifluorescence Axiovert 200M equipped with a Zeiss LSM 510 Meta confocal laser scanning microscope (Zeiss, Jena, Germany) and a LD C-Apochromat 40x/1.1 W Korr UV-VIS-IR water immersion objective (Zeiss). YG-PS NPs were excited with the 488 nm line of a 30 mW air-cooled argon ion laser (tube current set at 5.9 A) under the control of an acoustic-optic modulator. WGA was excited using a 543 nm helium neon laser. DAPI was excited using 150 fs pulsed laser light of a Ti:Sapphire laser (MaiTai, Spectra-Physics, Utrecht, The Netherlands) tuned at an output wavelength of 730 nm. The excitation light was directed to the sample through

a dichroic beam splitter (HFT UV/488/543/633). For the detection and separation of the different emitted fluorescence signals, a secondary dichroic beam splitter NFT 490 or NFT 545, as well as three band-pass filters BP 390-465 (DAPI), BP500-530 (YG-PS NPs), or BP565-615 (WGA) were used. Signals were directed towards an internal analog PMT (Zeiss).

Cell viability and proliferation

Cytotoxicity of the YG-PS NPs was assessed after 24 hours of cell exposure using Annexin V staining (Life Technologies) according to the manufacturer's protocol. Percentage positive cells was determined by flow cytometry. Staurosporine (0.1 µM, Sigma-Aldrich) was used as a positive control for programmed cell death. Cell proliferation was determined by counting the live cells at different time points using NucleoCassette™ and NucleoCounter® (ChemoMetec, Allenød, Denmark) for HPCs, and trypan blue exclusion (Invitrogen) using a Bürker counting chamber for CD34-DCs.

Results

Nanoparticle characterization

Fluorescently labelled, carboxylated YG-PS NPs with a nominal diameter of 40 nm were used in the present study. Before interaction with cells, proteins and electrolytes present within the cell culture medium may influence the intrinsic physicochemical parameters of the NPs used. Therefore, characterization of YG-PS NPs dispersions in both water and CCM after different incubation periods was performed by means of NTA (Figure 1). NP hydrodynamic diameter increased immediately from 50 ± 1 nm to 65 ± 5 nm when diluted in CCM due to adhering biomolecules. The resulting YG-PS NPs dispersions remained stable over the duration of the experiment. No signs of agglomeration or an increase of the biomolecular corona over time were found up to 96 hours. The zeta potential of YG-PS NPs reached a value close to neutrality when dispersed in CCM (from -40 ± 1 mV in water to 2 ± 3 mV in CCM).

Transient nanoparticle loading in HPCs

The interaction of HPCs with NPs was evaluated by exposing the cells to a concentration range of fluorescently labelled YG-PS NPs ranging from 5 to 90 µg ml^{-1}. After 24 hours of continuous exposure, the cellular NP load was evaluated by means of the geometric mean fluorescence intensity (GMFI) measured using flow cytometry (Figure 2A). HPCs displayed an almost linear loading profile with increasing NP concentration similar to CD34-DCs. However, compared to the differentiated CD34-DCs (Figure 2B), HPCs had a smaller NP loading capacity. As HPCs are non-phagocytic cells and have a lower cytoplasmic-to-nuclear ratio, they are expected to be less efficient in engulfing large amounts of extracellular material, such as NPs, than DCs with a prominent phagocytic activity.[20] In order to confirm if the processing of NPs is different by both cell types, the interaction of HPCs and CD34-DCs with NPs was studied as a function of time. The NP load was measured after 1, 2, 3, 4, 5, 6, and 24 hours of exposure to 50 µg ml^{-1} YG-PS NPs (Figure 2C, Figure 2D).

This concentration was chosen because it is still in the (almost) linear range of the concentration-response profile of HPCs while resulting in a strong signal. Surprisingly, within the first hour after exposure, both HPCs and CD34-DCs promptly accumulated NPs at a comparable rate. In CD34-DC the NP load continued to increase up to 24 hours post-exposure in a linear behavior/fashion, similar to what has been published previously for cancer cell lines.[7,21] HPCs, however, reached their maximum NP load within one hour of exposure, declining to a stationary state afterwards. Similar observations of decreasing cell-associated YG-PS NPs fluorescence were made using confocal microscopy analyses (Figure 3). Although HPCs obtained from different donors reveal variation in the absolute maximum fluorescence intensity, all samples demonstrated this transient loading.

Energy-dependent loading of HPCs and CD34-DCs with nanoparticles

The NP load of the cells could accumulate in several ways. Discrimination between passive or active processes can be made by performing the NP exposure of the cells at 4°C. This is a common way to assess the involved mechanisms as cooling down the cells inhibits all energy-dependent cellular processes.[22] Pre-incubation at 4°C for 1 hour and exposure of HPCs and CD34-DCs to 50 µg ml^{-1} YG-PS NPs also at 4°C strongly abolished the loading with YG-PS NPs. This was even more obvious when comparing the acquired load with the load accumulated by their cellular counterparts obtained from the same donors but exposed at 37°C (Figure 4A, Figure 4B). This unambiguously demonstrates that the loading process is an active process.
In addition, cells were exposed to 50 µg ml^{-1} YG-PS NPs for one hour at 37°C and cooled down to 4°C in the presence of YG-PS NPs in order to reveal whether the apparent YG-PS NP release process in HPCs is energy-dependent (Figure 4C, Figure 4D). Although HPCs at 37°C showed a strong decline in GMFI, cooling down to 4°C completely blocked this process resulting in a constant load. These results clearly demonstrate that both the loading and release processes in HPCs are energy-dependent. Moreover, these observations suggest that an arrest of NP loading occurs over time, or that the release rate of NPs changes over time, or that the signal from the YG-PS NPs declines during the course of the measurement, or a combination of these processes.

The observed transient loading cannot be ascribed to the fluorescent staining of the nanoparticles

In order to support the hypothesis of NP release by HPCs, additional experiments were performed to exclude technical artefacts in the experimental design. A widespread problem with the usage of fluorescently labelled NPs is the presence of residual free dye or labile dye which represents dye leaching out of the NPs. [7,23] This could confound the obtained results in HPCs but seems, however, not to agree with the results observed in CD34-DCs.

In order to characterize the interference by dye leaching, dialysis experiments were performed to determine the extent of free dye under the experimental conditions.

NPs are recognized to enter mammalian cells through the endocytosis mechanism.[24,25] NPs' journey through the endocytic compartment corresponds with an acidification of the NPs' environment. The endosomal acidification was mimicked here by dispersing the YG-PS NPs in a citric acid – phosphate buffer having a pH of 5, 6 or 7, which corresponds to the pH within the endolysosomal compartment.[26] Thereafter, YG-PS NPs dispersions were dialyzed against citric acid – phosphate buffers with different acidity. YG-PS NPs stock dispersions were used as purchased (stock YG-PS NPs) or pre-dialyzed for 48 hours to remove all labile dye already present in the NPs dispersions (pre-dialyzed YG-PS NPs). The time kinetics of the dialyses was measured using fluorescence spectroscopy (Figure S2).

Approximately 10% of free or labile dye was present in the YG-PS NP stock solutions. Pre-dialysis of the YG-PS NP stock solutions, however, was not effective in reducing the further release of labile or free dye in the dialysate. No significant effect of acidification on leaching was found. To assess the potential impact of free dye on the observed interaction kinetics of the NPs in HPCs, cells were exposed to the free dye present in the dialysate after 48 hours of dialysis at 37°C and 5% CO_2, or to corresponding amount of YG-PS NPs (Figure S3). The free dye only comprised a small portion of the total fluorescence intensity compared to the YG-PS NPs, which remained rather stable in function of the time. These data suggest minor impact of the free dye on the observed time kinetics of YG-PS NPs in HPCs.

To investigate possible pH-dependent changes in the fluorescence properties of the dyes embedded within or attached to the YG-PS NPs fluorescence lifetime spectroscopy experiments were performed. The mean recovered fluorescence lifetime did not alter within the tested pH range of pH 5 to 7, indicating no significant change in the fluorescence properties of the fluorophores (Figure S4, Table S1).

Since YG-PS NPs loading and release were shown to be strongly reduced when incubated at 4°C, the effect of temperature on the presence and release of labile and free dye was determined. This was achieved by dialysis at 4°C and compared to 37°C against a citric acid –

phosphate buffer of pH 7 (data not shown). A slight difference between both conditions was found with 8% versus 12% of labile or free dye determined after 24 hours of dialysis at 4°C and 37°C respectively. These findings demonstrate that the arrest of the release phenomenon of HPCs due to cooling down to 4°C cannot be accredited to labile and free dye alone. As incubation of YG-PS NPs at 4°C slows down the leaching only minimally, it would not be sufficient to retain the decay in GMFI of HPCs when the observed release process was due to a passive diffusion process such as dye leaching.

Negligible cell death and proliferation of HPCs and CD34-DC upon nanoparticle exposure

Cytotoxic effects as well as cell proliferation, in which the NP load will be divided over the daughter cells, could be another cause of the observed decrease of NP load.[7,21] In order to investigate the presence of cytotoxicity, an Annexin V staining was performed after 24 hours of exposure to different doses of YG-PS NPs. In addition, the live cell number was determined in both HPCs and CD34-DCs (Figure 5). No increased apoptosis was found for both cell types. Cell counting indicated a modest increase in cell proliferation for both cell types after 24 hours, however, this was not observed in the time window where the most release was observed (eg 2-4 hours). Therefore, it is reasonable to conclude that the observed transient load is not a consequence of these processes.

Modelling the kinetics of cellular nanoparticle load

The dynamics of YG-PS NPs in HPCs can be easily described mathematically. Denote the cellular NP load by the number of particles *N*, which is proportional to the experimental fluorescent signal measured by the flow cytometer (GMFI). To model the kinetics of *N* we assume that cell proliferation and cell death can be neglected, which is realistic for the experiments with HPCs and also for shorter time scales of CD34-DCs (Figure 5). Then, the time dependence of *N* is determined by two competing contributions: a positive contribution due to the uptake of NPs from the extracellular medium increasing the cellular NP load and a negative contribution due to

NPs released from the cell and entering the medium again. In its most simple form the time derivative of *N* can be modeled by:

$$\frac{dN}{dt} = R_{on}.c - R_{off}.N \qquad \text{(Eq. 1)}$$

in which *c* is the extracellular NP concentration, assumed to be a reservoir and hence constant, R_{on} and R_{off} are the rates of the competing processes.

If R_{on} is constant and R_{off} is zero, there is no NP release and *N* increases linearly in time. This behavior is essentially observed in the CD34-DCs (Figure 2D) and many cell lines for short time scales.[7] Our experiments with HPCs exhibit clearly a different time dependent loading (Figure 2C), suggesting the presence of a release process, ie a positive R_{off} value with a NP release proportional to the load *N*. In this case the cellular NP load will experience a decreasing growth and will eventually saturate at a dynamic steady-state. However, if R_{off} is assumed to be a constant value, ie time-independent, *N* will be a monotonic function of time, which is clearly not what we observe. Our experiments show that the load *N* peaks within a time frame of one hour and decreases afterwards (Figure 2C). This suggests an active response in which the release rate increases over time. The experimental behavior can be modelled by (Eq. 1) if we assume a time dependent R_{off} rate (Figure 6A).Figure 6B shows the estimations of R_{off} based on (Eq. 1) in which the time derivative is approximated by the finite time difference determined by the experimental measurement frequency. This time dependence can be used to numerically solve differential (Eq. 1) and it results in the simulated load presented inFigure 6A. This first model approach indicates that the release rate of the YG-PS NPs increases in time; this result is rather robust and remains present also when eg a fixed background signal is subtracted from the NP load signal for instance due to the adhesion of NPs to the cell membrane.

Discussion

In the present study the interaction kinetics of carboxylated YG-PS NPs in HPCs and CD34-DCs were observed to respond differently to identical NPs and under identical conditions. HPCs showed a transient association with the YG-PS NPs, whereas the CD34-DCs displayed a

monotonic increase of NP load over time. This can partially be explained by the difference in their cell physiology. CD34-DCs are more confined to and involved in antigen presentation and immune responses,[18] whereas HPCs' main ability is to self-renew or multiply.[1] The differences in cell physiology are coupled with morphological differences. HPCs derived from cord blood have a high nucleus-cytoplasm ratio, with the cytoplasm poor in organelles, although a few mitochondria and endoplasmic reticulum cisternae can be seen.[20] In contrast, CD34-DCs have a relatively lower nucleus/cytoplasm ratio, and thus, a cytoplasm containing significantly more organelles including endosomal vesicles.[27] The observations made in this study corroborate the involvement of active cellular processes in the newly observed transient load of HPCs. To our knowledge, this is the first time that this transient loading behavior of HPCs with YG-PS NPs has been reported. Brüstle *et al* demonstrated the interaction of HPCs and PS NPs, where the uptake of 120-nm sized carboxylated PS NPs was evaluated after 24 hours of exposure and showed the presence of intracellular vesicles containing NPs.[28] *Duinhouwer et al* showed uptake of PGLA NPs in HPCs after 4 and 20 hours of exposure, without affecting their proliferation and differentiation capabilities.[29] Other studies in which iron oxide and Gd_2O_3 NPs by HPCs were used for MRI applications have reported solely their uptake and little effect on cellular function.[9-11,30,31] None of these preceding studies have reported the short-time kinetics of NPs in HPCs. Transient loading of cells requires the release of the NPs, as we have described using the physics model. NP release has been reported before in multiple cell types and reviewed by *Sakhtianchi et al* and *Oh et al*. [25,32] Internalized NPs are often delivered in early endosomes, which are considered as the main sorting station of the endocytic machinery.[33,34] Although the majority of the NPs reside in the endolysosomal pathways, a fraction of the NPs is capable to escape to recycling endosomes and is eventually released by cells.[35,36] The NPs that are trapped in the endocytic machinery will end up in the lysosomal compartments. Some of the lysosomes are capable in undergoing exocytosis through fusion with the plasma membrane.[37,38] In addition, NPs that have entered the endoplasmic reticulum of the Golgi apparatus may leave cells via vesicles related to the secretion system.[39] Also NPs that are present in the cytoplasm (eg NP uptake by diffusion or endolysosomal escape of NPs) can leave the cell as well through re-entry to the vesicular system

or via unspecific mechanisms.[32,37] Based on these reports, it is conceivable to have also an active release in HPCs.

Maintaining and characterizing the physical and chemical stability of NPs is a crucial requirement for correctly assessing their biological effects. Instability of the NPs can result in altered nano-bio interactions, and also complicates the interpretation of their outcome. Evaluating the uptake and release of NPs using fluorescence-based techniques is often problematic by the presence of residual free dye or labile dye within the NP dispersion.[7,23] It is very difficult to establish whether the observed phenomenon in HPCs is solely attributed to a specific cellular behavior because of the possibility of technical artefacts which may influence the observations and the limitations of the available techniques. Although flow cytometry has proven its value in many NP uptake studies, the presence of residual free dye can strongly influence the NP uptake profile.[7,23] Confocal laser scanning microscopy cannot distinguish free dye from YG-PS NPs. Moreover, as the HPCs are relatively small and have a high nucleus-to-cytoplasm volume ratio, the diffraction-limited resolution of a confocal microscope does not allow determining the difference between internalized NPs or NPs associated with the cell membrane due to the small cytoplasm of the HPCs. In order to explore whether a significant proportion of the dye was released from the PS NPs under biological conditions, HPCs and CD34-DCs were exposed under energy-depleted conditions. These experiments demonstrated that the loading and/or release of YG-PS NPs were energy-dependent. This cannot be explained when the observed process was purely credited to dye leaching and diffusion of the labile dye from the NPs. Moreover, the transient behavior was not attributed to HPCs proliferation in which NPs divide over the daughter cells or through the induction of apoptotic cell death in which the NPs may leave the cell through the release of apoptotic bodies. In order to exclude that the observed transient loading behavior of HPCs was caused through dye leaching, the extent of free dye or labile dye present in the NP mixture was determined through dialysis experiments under the experimental conditions (ie in a pH range between 5 and 7 analogous to the acidity of the endolysosomal compartment and cell culture medium, respectively). A limited amount of free dye was present in the dialysate of the NPs' stock solution, which was independent from the pH of the solution. We demonstrated that the free dye

only comprised a small fraction of the total fluorescence intensity compared to the fluorescence intensity obtained when cells were exposed to YG-PS NPs. Moreover, the intensity profile remained rather stable as a function of time. These results suggest that the impact of residual free dye or labile dye on the cells is rather limited. Nevertheless, it is very difficult to establish this without any doubt as in some reports it has been demonstrated that polymeric NPs which do not appear to leach under aqueous solutions in contrary can leach dye when their become in contact with the hydrophobic environment of the cell.[7,23,40]

In order to validate if there is indeed NP internalization and an active excretion of the YG-PS NPs by HPCs over time, the intracellular and time-dependent YG-PS NPs content should ideally be monitored. Electron microscopy is frequently used to demonstrate the intracellular localization of NPs, however, as YG-PS NPs are lucent under these conditions they can be confused with spherical vesicular structures with the risk that changes in cellular structures are mistaken for changes in the intracellular accumulation of YG-PS NPs in HPCs.[41] Moreover, as YG-PS NPs are composed of organic materials, they cannot be measured using ICP-MS analysis. For that reason, it is highly necessary that our observations are being reproduced with other NPs having a similar size, charge and protein corona composition, but different core which allows validating the observation of NP release using other, more direct quantitative approaches such as ICP-MS or electron microscopy.

Conclusion

Therapeutic strategies and transplantations using HSCs and HPCs may benefit from their remarkable response to YG-PS NPs. The observed transient loading mechanism can open new opportunities for the safe delivery of drugs or molecules of interest with limited bio-accumulation. However, further investigation is required to further explore whether the observed phenomenon is specific for the NPs used. The effects of NP species, size, functionalization, administered dose, incubation time and intracellular fate should be carefully investigated. Moreover, more research is needed as well to reveal how HPCs are capable in mediating the release and which cellular

functions and associated dynamics are involved in this process. The resulting knowledge will allow us to exploit the full potential of NP applications in medicine.

Acknowledgments

The authors would like to thank Birgit Baré and Pascale Berckmans for their contribution in the flow cytometry experiments. This work was funded by INTERREG-IV A (BioMiMedics), BOF (Hasselt University), a tUL impulse grant Phase II by the Province of Limburg (Belgium), FP7 project QualityNano [Grant Agreement N° INFRA-2010-262163]. Sarah Deville was supported by a fellowship of VITO and Hasselt University (BOF). Nick Smisdom was supported by a post-doctoral scholarship of Research Foundation Flanders (FWO Vlaanderen) and VITO. Bart Wathiong was supported by a fellowship of VITO.

Disclosure

The author reports no conflicts of interest in this work.

References

1. Woods NB, Ooka A, Karlsson S. Development of gene therapy for hematopoietic stem cells using lentiviral vectors. *Leukemia.* 2002;16(4):563-569.
2. Edmundson M, Thanh NT, Song B. Nanoparticles based stem cell tracking in regenerative medicine. *Theranostics.* 2013;3(8):573-582.
3. Lu R, Neff NF, Quake SR, Weissman IL. Tracking single hematopoietic stem cells in vivo using high-throughput sequencing in conjunction with viral genetic barcoding. *Nat Biotechnol.* 2011;29(10):928-933.
4. Kay MA. State-of-the-art gene-based therapies: the road ahead. *Nat Rev Genet.* 2011;12(5):316-328.

5. Stuckey DW, Shah K. Stem cell-based therapies for cancer treatment: separating hope from hype. *Nat Rev Cancer.* 2014;14(10):683-691.

6. Kim JA, Aberg C, de Carcer G, Malumbres M, Salvati A, Dawson KA. Low Dose of Amino-Modified Nanoparticles Induces Cell Cycle Arrest. *ACS Nano.* 2013.

7. Salvati A, Åberg C, dos Santos T, et al. Experimental and theoretical comparison of intracellular import of polymeric nanoparticles and small molecules: toward models of uptake kinetics. *Nanomedicine.* 2011;7(6):818-826.

8. Lee DE, Koo H, Sun IC, Ryu JH, Kim K, Kwon IC. Multifunctional nanoparticles for multimodal imaging and theragnosis. *Chem Soc Rev.* 2012;41(7):2656-2672.

9. England TJ, Bath PM, Abaei M, Auer D, Jones DR. Hematopoietic stem cell (CD34+) uptake of superparamagnetic iron oxide is enhanced by but not dependent on a transfection agent. *Cytotherapy.* 2013;15(3):384-390.

10. Daldrup-Link HE, Rudelius M, Oostendorp RA, et al. Targeting of hematopoietic progenitor cells with MR contrast agents. *Radiology.* 2003;228(3):760-767.

11. Daldrup-Link HE, Rudelius M, Piontek G, et al. Migration of iron oxide-labeled human hematopoietic progenitor cells in a mouse model: in vivo monitoring with 1.5-T MR imaging equipment. *Radiology.* 2005;234(1):197-205.

12. Hedlund A, Ahren M, Gustafsson H, et al. Gd(2)O(3) nanoparticles in hematopoietic cells for MRI contrast enhancement. *Int J Nanomedicine.* 2011;6:3233-3240.

13. McNeer NA, Chin JY, Schleifman EB, Fields RJ, Glazer PM, Saltzman WM. Nanoparticles deliver triplex-forming PNAs for site-specific genomic recombination in CD34+ human hematopoietic progenitors. *Mol Ther.* 2011;19(1):172-180.

14. McNeer NA, Schleifman EB, Cuthbert A, et al. Systemic delivery of triplex-forming PNA and donor DNA by nanoparticles mediates site-specific genome editing of human hematopoietic cells in vivo. *Gene Ther.* 2013;20(6):658-669.

15. Mottram PL, Leong D, Crimeen-Irwin B, et al. Type 1 and 2 immunity following vaccination is influenced by nanoparticle size: formulation of a model vaccine for respiratory syncytial virus. *Mol Pharm.* 2007;4(1):73-84.

16. Fifis T, Gamvrellis A, Crimeen-Irwin B, et al. Size-dependent immunogenicity: therapeutic and protective properties of nano-vaccines against tumors. *J Immunol.* 2004;173(5):3148-3154.

17. Varela JA, Bexiga MG, Aberg C, Simpson JC, Dawson KA. Quantifying size-dependent interactions between fluorescently labeled polystyrene nanoparticles and mammalian cells. *J Nanobiotechnology.* 2012;10:39.

18. Diwan M, Elamanchili P, Lane H, Gainer A, Samuel J. Biodegradable nanoparticle mediated antigen delivery to human cord blood derived dendritic cells for induction of primary T cell responses. *Journal of drug targeting.* 2003;11(8-10):495-507.

19. Schoeters E, Verheyen GR, Nelissen I, et al. Microarray analyses in dendritic cells reveal potential biomarkers for chemical-induced skin sensitization. *Mol Immunol.* 2007;44(12):3222-3233.

20. Deliliers GL, Caneva L, Fumiatti R, et al. Ultrastructural Features of CD34+ Hematopoietic Progenitor Cells from Bone Marrow, Peripheral Blood and Umbilical Cord Blood. *Leuk Lymphoma.* 2001;42(4):699-708.

21. Kim JA, Aberg C, Salvati A, Dawson KA. Role of cell cycle on the cellular uptake and dilution of nanoparticles in a cell population. *Nat Nanotechnol.* 2012;7(1):62-68.

22. Rode M, Berg T, Gjøen T. Effect of Temperature on Endocytosis and Intracellular Transport in the Cell Line SHK-1 Derived from Salmon Head Kidney. *Comp Biochem Physiol A Mol Integr* 1997;117(4):531-537.

23. Tenuta T, Monopoli MP, Kim J, et al. Elution of Labile Fluorescent Dye from Nanoparticles during Biological Use. *PloS one.* 2011;6(10):e25556.

24. Iversen T-G, Skotland T, Sandvig K. Endocytosis and intracellular transport of nanoparticles: Present knowledge and need for future studies. *Nano Today.* 2011;6(2):176-185.

25. Oh N, Park J-H. Endocytosis and exocytosis of nanoparticles in mammalian cells. *Int J Nanomedicine.* 2014;9(Suppl 1):51-63.

26. Hara-Chikuma M, Yang B, Sonawane ND, Sasaki S, Uchida S, Verkman AS. ClC-3 chloride channels facilitate endosomal acidification and chloride accumulation. *The Journal of biological chemistry.* 2005;280(2):1241-1247.

27. Clark EM, Joshi DS, Grimm AB, Joshi AD, Wang P, Joshi SS. Ultrastructural basis of enhanced antitumor cytotoxicity of cord blood-derived CTLs: a comparative analysis with peripheral blood and bone marrow. *Int J Oncol.* 2010;37(3):645-653.

28. Brüstle I, Simmet T, Nienhaus GU, Landfester K, Mailänder V. Hematopoietic and mesenchymal stem cells: polymeric nanoparticle uptake and lineage differentiation. *Beilstein J Nanotechnol.* 2015;6:383-395.

29. Duinhouwer LE, van Rossum BJM, van Tiel ST, et al. Magnetic Resonance Detection of CD34+ Cells from Umbilical Cord Blood Using a 19-F Label. *PloS one.* 2015;10(9):e0138572.

30. Maxwell DJ, Bonde J, Hess DA, et al. Fluorophore-conjugated iron oxide nanoparticle labeling and analysis of engrafting human hematopoietic stem cells. *Stem Cells.* 2008;26(2):517-524.

31. Arbab AS, Yocum GT, Rad AM, et al. Labeling of cells with ferumoxides-protamine sulfate complexes does not inhibit function or differentiation capacity of hematopoietic or mesenchymal stem cells. *NMR Biomed.* 2005;18(8):553-559.

32. Sakhtianchi R, Minchin RF, Lee KB, Alkilany AM, Serpooshan V, Mahmoudi M. Exocytosis of nanoparticles from cells: role in cellular retention and toxicity. *Adv Colloid Interface Sci.* 2013;201-202:18-29.

33. dos Santos T, Varela J, Lynch I, Salvati A, Dawson KA. Effects of transport inhibitors on the cellular uptake of carboxylated polystyrene nanoparticles in different cell lines. *PLoS One.* 2011;6(9):e24438.

34. dos Santos T, Varela J, Lynch I, Salvati A, Dawson KA. Quantitative Assessment of the Comparative Nanoparticle-Uptake Efficiency of a Range of Cell Lines. *Small.* 2011;7(23):3341-3349.

35. Stayton I, Winiarz J, Shannon K, Ma Y. Study of uptake and loss of silica nanoparticles in living human lung epithelial cells at single cell level. *Anal Bioanal Chem.* 2009;394(6):1595-1608.

36. Chu Z, Huang Y, Tao Q, Li Q. Cellular uptake, evolution, and excretion of silica nanoparticles in human cells. *Nanoscale.* 2011;3(8):3291-3299.

37. Panyam J, Labhasetwar V. Dynamics of endocytosis and exocytosis of poly(D,L-lactide-co-glycolide) nanoparticles in vascular smooth muscle cells. *Pharm Res.* 2003;20(2):212-220.

38. Jiang X, Rocker C, Hafner M, Brandholt S, Dorlich RM, Nienhaus GU. Endo- and exocytosis of zwitterionic quantum dot nanoparticles by live HeLa cells. *ACS Nano.* 2010;4(11):6787-6797.

39. Cartiera MS, Johnson KM, Rajendran V, Caplan MJ, Saltzman WM. The uptake and intracellular fate of PLGA nanoparticles in epithelial cells. *Biomaterials.* 2009;30(14):2790-2798.

40. Pietzonka P, Rothen-Rutishauser B, Langguth P, Wunderli-Allenspach H, Walter E, Merkle HP. Transfer of lipophilic markers from PLGA and polystyrene nanoparticles to caco-2 monolayers mimics particle uptake. *Pharm Res.* 2002;19(5):595-601.

41. Mühlfeld C, Rothen-Rutishauser B, Vanhecke D, Blank F, Gehr P, Ochs M. Visualization and quantitative analysis of nanoparticles in the respiratory tract by transmission electron microscopy. *Part Fibre Toxicol.* 2007;4(1):1-17.

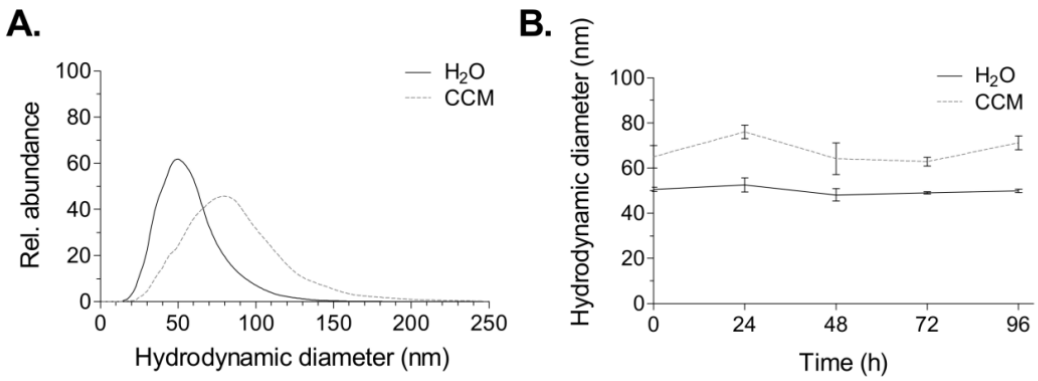

Figure 1: YG-PS NPs in cell culture conditions (50 µg/ml) acquire a biomolecular corona and remain colloidally stable. (a) Size distribution of YG-PS NPs after 24 hours of incubation at 37 °C and 5% CO_2 respectively in H_2O and CCM. The NP hydrodynamic diameter increased from 50 ± 1 nm to 76 ± 3 nm when dispersed in CCM. (b) The hydrodynamic diameter does not change over time, indicating a stable dispersion. *All sizes are reported as the mean ± SEM of the mode of NP hydrodynamic diameter distributions obtained from 3 replicates.*

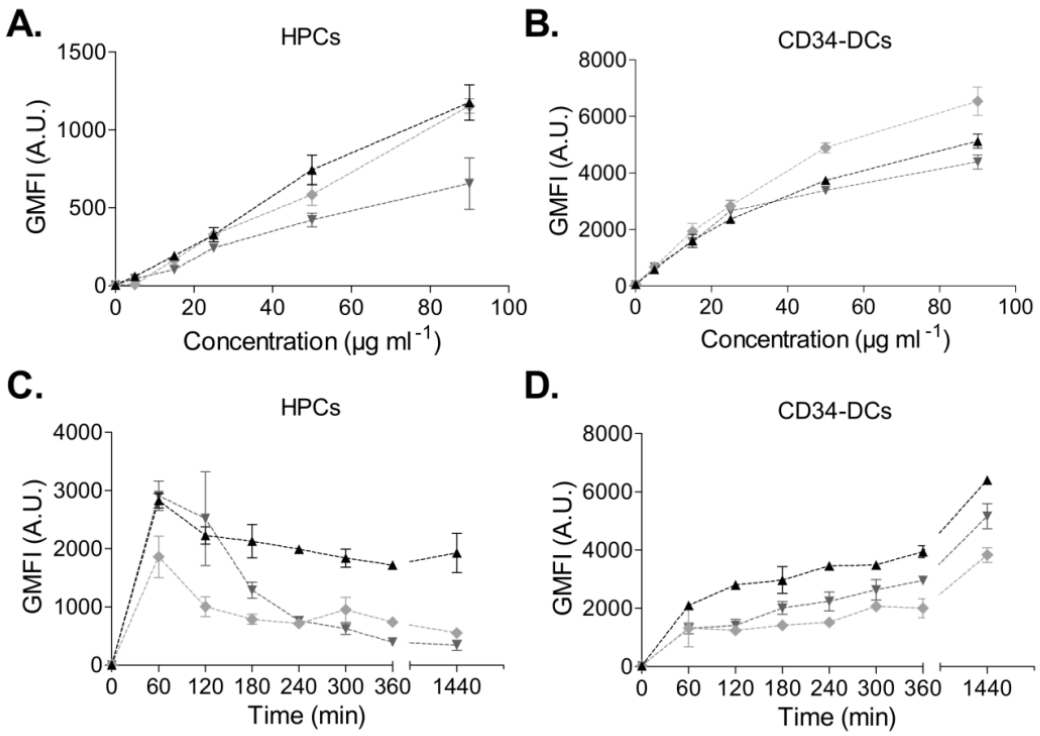

Figure 2: CD34^{+} HPCs show reversible association with 40-nm sized carboxylated YG-PS NPs, a behavior lost in HPC-derived CD34-DCs. Dose-dependent loading of HPCs (A) and CD34-DCs (B) after 24 hours of exposure to fluorescent 40-nm sized carboxylated YG-PS NPs. The GMFI of CD34-DCs is larger than the GMFI of HPCs, as expected from the lower cytoplasm-to-nucleus ratio of the latter. In addition, a remarkable discrepancy is observed between the time evolution of NP processing by HPCs (C) and CD34-DCs (D). When exposed to 50 µg ml^{-1} fluorescent 40-nm sized carboxylated YG-PS NPs, HPCs display a transient increase in GMFI in contrast to the steady and continuous increase observed in CD34-DCs. *All values are reported as the mean ± standard derivation (SD) of 3 technical replicates. Different curves represent independent biological experiments from different donors.*

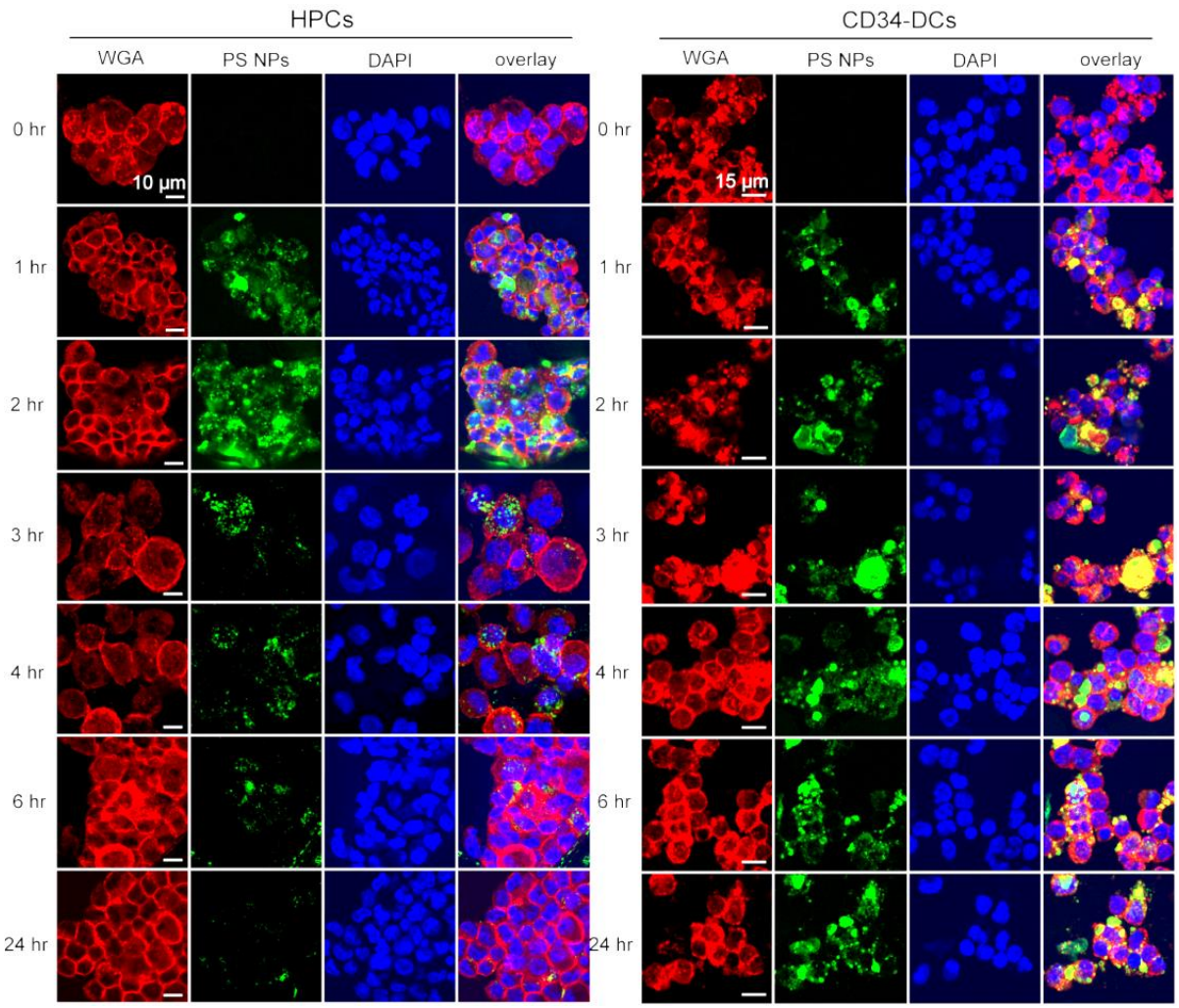

Figure 3: Uptake kinetics of 40-nm sized carboxylated YG-PS NPs in HPCs and CD34-DCs. Microscopy images of time kinetics after exposure to 50 µg ml^{-1} uptake YG-PS NPs (green). Nuclei of cells are labelled with DAPI (blue) and cell membranes labelled with Alexa Fluor® 555 conjugated WGA (red).

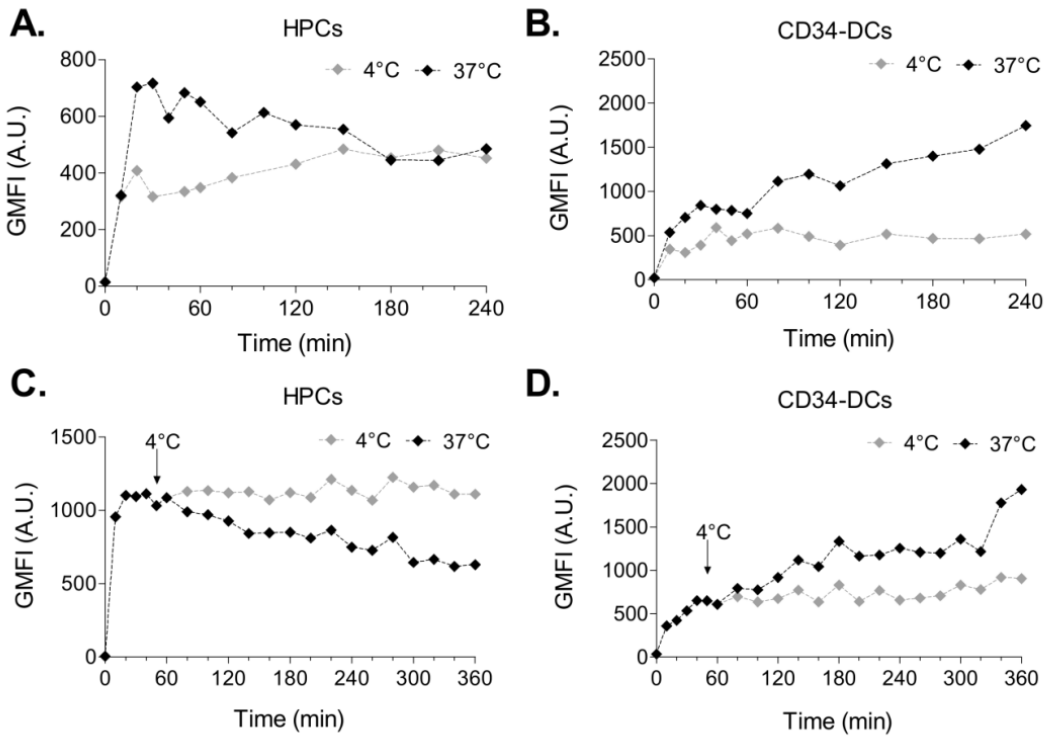

Figure 4: YG-PS NPs loading and release are energy-dependent. The loading with fluorescent 40-nm YG-PS NPs is energy-dependent in both HPCs (A) and CD34-DCs (B). Cells were incubated for one hour at 37°C or 4°C prior to exposure to 50 µg ml^{-1} uptake YG-PS NPs at the same temperature. Furthermore, energy-dependent release of NPs is demonstrated in HPCs (C), while CD34-DCs continue to accumulate NPs (D). Here, cells were exposed to 50 µg ml^{-1} YG-PS NPs at 37°C and after 1 hour cells were cooled down to 4°C to block all active processes. *Different curves represent different treatment conditions of cells from one single donor. For every panel a representative example from two independent donors is shown (independent experimental data obtained from the other donor are found in Figure S1).*

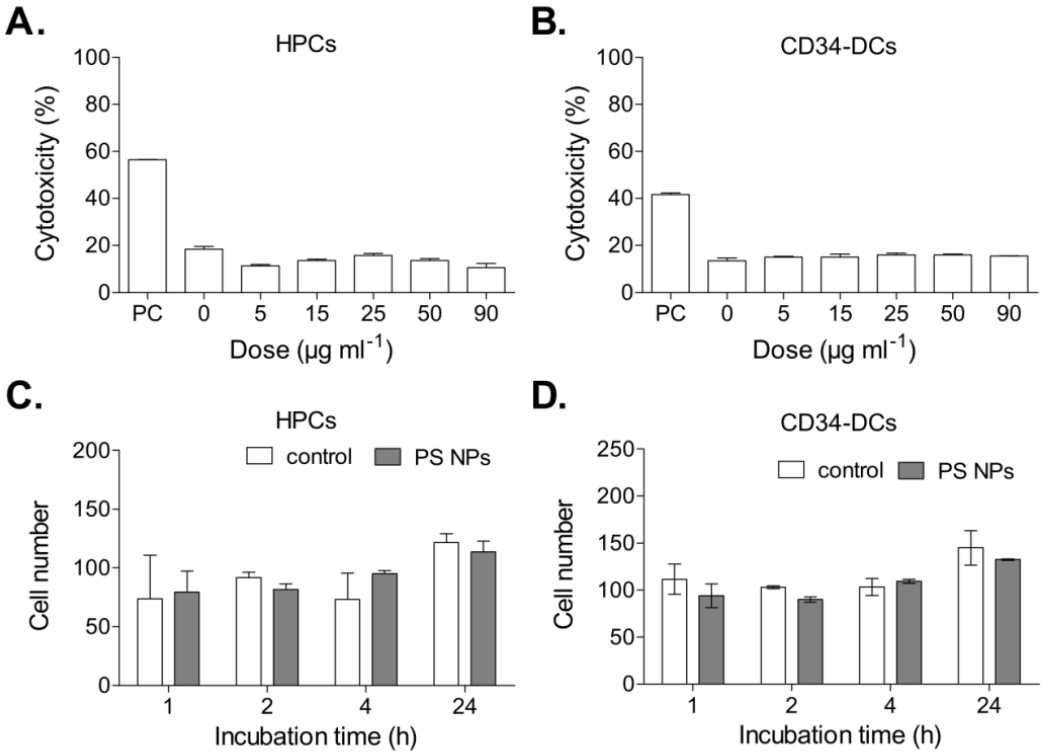

Figure 5: Assessment of apoptosis and cell proliferation of HPCs and CD34-DCs after exposure to 40-nm carboxylated YG-PS NPs. HPCs (A) and CD34-DCs (B) were exposed for 24 hours to YG-PS NPs at 37°C and evaluated for induction of apoptosis using Annexin V staining. Staurosporine (0.1 µM) was used as a positive control (PC). The mean ± SD of technical replicates (HPCs n=2; CD34-DC n=3) are shown. (C-D) Cell counting indicated a modest increase in the total cell number during the experimental time. Representative examples for HPCs (C) and CD34-DCs (D) are shown, with and without exposure to 50 µg ml^{-1} YG-PS NPs. Mean values ± SD of 2 technical replicates.

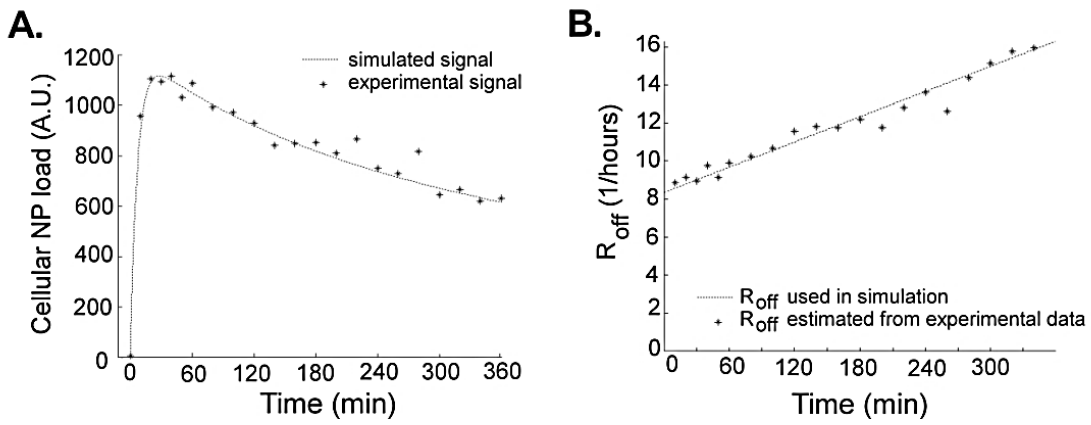

Figure 6: Model of the cellular load kinetics of YG-PS NPs in HPCs describing the presence of a release process. The simulated and the experimentally obtained values of (a) the cellular NP load as a response to an exposure at a fixed NP concentration starting at time zero. (b) The release rate R_{off} as a function of time.